

# *Impact of ocean resolution on coupled air-sea fluxes and large-scale climate*

Article

Published Version

Roberts, M. J., Hewitt, H. T., Hyder, P., Ferreira, D. ORCID: <https://orcid.org/0000-0003-3243-9774>, Josey, S. A., Mizieliński, M. and Shelly, A. (2016) Impact of ocean resolution on coupled air-sea fluxes and large-scale climate. *Geophysical Research Letters*, 43 (19). 10,430-10,438. ISSN 0094-8276 doi: 10.1002/2016GL070559 Available at <https://centaur.reading.ac.uk/66798/>

It is advisable to refer to the publisher's version if you intend to cite from the work. See [Guidance on citing](#).

To link to this article DOI: <http://dx.doi.org/10.1002/2016GL070559>

Publisher: American Geophysical Union

All outputs in CentAUR are protected by Intellectual Property Rights law, including copyright law. Copyright and IPR is retained by the creators or other copyright holders. Terms and conditions for use of this material are defined in the [End User Agreement](#).

[www.reading.ac.uk/centaur](http://www.reading.ac.uk/centaur)

**CentAUR**

Central Archive at the University of Reading

Reading's research outputs online

## RESEARCH LETTER

10.1002/2016GL070559

## Key Points:

- Demonstrate that eddy-permitting is sufficient to capture observed temporal relationship between SST, wind stress over boundary currents
- Eddy-resolving resolution improves mean state of fluxes and leads to changes in large-scale modeled heat transport
- Benefits of high ocean resolution improving mean state may be more important than direct influence of changes to air-sea interactions

## Supporting Information:

- Supporting Information S1

## Correspondence to:

M. J. Roberts,  
malcolm.roberts@metoffice.gov.uk

## Citation:

Roberts, M. J., H. T. Hewitt, P. Hyder, D. Ferreira, S. A. Josey, M. Mizielinski, and A. Shelly (2016), Impact of ocean resolution on coupled air-sea fluxes and large-scale climate, *Geophys. Res. Lett.*, 43, 10,430–10,438, doi:10.1002/2016GL070559.

Received 22 JUL 2016

Accepted 9 SEP 2016

Accepted article online 12 SEP 2016

Published online 13 OCT 2016

## Impact of ocean resolution on coupled air-sea fluxes and large-scale climate

Malcolm J. Roberts<sup>1</sup>, Helene T. Hewitt<sup>1</sup>, Pat Hyder<sup>1</sup>, David Ferreira<sup>2</sup>, Simon A. Josey<sup>3</sup>, Matthew Mizielinski<sup>1</sup>, and Ann Shelly<sup>1,4</sup>
<sup>1</sup>Met Office, Exeter, UK, <sup>2</sup>Department of Meteorology, University of Reading, Reading, UK, <sup>3</sup>National Oceanography Centre, Southampton, UK, <sup>4</sup>Now at Cumulus, City Financial Investment Company Limited, London, UK

**Abstract** Air-sea fluxes are a crucial component in the energetics of the global climate system. The largest air-sea fluxes occur in regions of high sea surface temperature variability, such as ocean boundary, frontal currents and eddies. In this paper we explore the importance of ocean model resolution to resolve air-sea flux relationships in these areas. We examine the sea surface temperature-wind stress relationship in high-pass filtered observations and two versions of the Met Office climate model with eddy-permitting and eddy-resolving ocean resolutions. Eddy-resolving resolution shows marginal improvement in the relationship over eddy-permitting resolution. However, by focussing on the North Atlantic we show that the eddy-resolving model has significant enhancement of latent heat loss over the North Atlantic Current region, a long-standing model bias. While eddy-resolving resolution does not change the air-sea flux relationship at small scale, the impact on the mean state has important implications for the reliability of future climate projections.

## 1. Introduction

Small-scale interactions between atmosphere and ocean, mediated via air-sea fluxes, have been shown to have large-scale implications for the climate system. *Minobe et al.* [2008] showed how Sea Surface Temperature (SST) gradients influence the deep atmosphere, while other studies [e.g., *Zhang and Vallis*, 2013] showed how such interactions affect penetration of heat into the ocean interior. The wind response to mesoscale SST is also coupled to other boundary layer changes such as clouds (via surface convergence), as noted by *Perlin et al.* [2014]. SST-induced wind stress curl changes can have important feedbacks to the ocean circulation via Ekman pumping [*Chelton et al.*, 2007]. *Chelton and Xie* [2010] have used observational data to demonstrate a quasi-linear relationship between small-scale SST and wind perturbations, providing an important metric for frontal and mesoscale processes.

*Kirtman et al.* [2012] have shown the existence of significant correlations between monthly mean anomalies of SST and turbulent heat fluxes in particular regions of the ocean, specifically near boundary currents, in the Southern Ocean and near the equator. They argue that in these regions the ocean is driving the atmospheric circulation through SST anomalies, with the mid-latitude correlations only becoming evident in an eddy-resolving ocean model compared to a 1° ocean. This implies that errors in either modeled SST or surface flux (and their variability) have the potential to cause systematic model biases.

Air-sea interactions pose a particular challenge to current climate models. They require both adequate resolutions of the small-scale structures such as the ocean boundary currents and eddies, as well as sufficiently long integrations to study the impacts on the large-scale circulation and energetics of the climate system. Studies such as *Bryan et al.* [2010] and *Small et al.* [2014] have shown how coupled models with eddy resolving ocean resolution (of around 1/10°) can improve the relationships between SST, wind and other atmospheric variables, though the strength of the modeled interactions tends to be weaker than that observed.

However, capturing these small-scale relationships should not undermine the need to also adequately represent the correct mean state surface heat flux. At equilibrium, this flux balances the ocean heat transport divergence. When coupling and surface fluxes are poorly represented in models, other aspects of the atmosphere-ocean-sea-ice system may be corrected in erroneous ways in order to ensure that aspects of the large-scale circulation (for example, ocean heat transport, meridional overturning, and atmospheric boundary layer processes) agree with observations. This is problematic when observational constraints are uncertain (such as in turbulent heat fluxes). Climate model mean state biases are such that it is extremely difficult (if not impossible) to simulate the correct fluxes, and hence, any aspects of the large-scale circulation driven by these fluxes will be degraded.

Most previous studies of air-sea processes have used a comparison between an ocean model in which eddies are wholly parameterized (of order  $1^\circ$ , typical of Coupled Model Intercomparison Project (CMIP)-class models), and one in which eddies are resolved (at least in many parts of the globe) [Hallberg, 2013] at  $\sim 1/10^\circ$ . Hence it is unclear whether the full eddy resolution is required, or if an eddy-permitting resolution ( $\sim 1/4^\circ$ ) may be adequate to represent these interactions. Although there are reasons why such resolutions are not ideal – significantly more expensive than  $1^\circ$ , uncertainty over how to represent sub-grid scale processes, and significantly lower eddy kinetic energy than observed – they do offer improved variability, including ocean eddies, and representation of crucial large-scale features such as boundary currents, leading to reductions in biases [Scaife *et al.*, 2011].

This work has used the first eddy-resolving global coupled simulation with the  $1/12^\circ$  NEMO ocean model coupled to 25 km atmosphere model (as described in Hewitt *et al.* [2016]) to study air-sea interactions over a 20 year timeframe. It is compared to a similarly configured model with an eddy-permitting  $1/4^\circ$  resolution. In section 2 we describe the experimental design, models, and observational datasets used in this study. In section 3 we describe our analysis of the relationships between high-pass filtered fields of SST, wind stress and latent heat following the work of Chelton *et al.* [2004], Chelton and Xie [2010], and Bryan *et al.* [2010], and link this to the relationship between monthly mean anomalies of SST and turbulent flux after Kirtman *et al.* [2012]. In section 4 we show how an improved mean state in the eddy-resolving ocean is crucial for the large-scale climate in the North Atlantic, via both improved latent heat fluxes and an enhanced boundary current. In section 5 we present our conclusions and discuss future avenues of research.

## 2. Methods

This study uses models documented extensively by Hewitt *et al.* [2016], and hence, only a short summary of the relevant details will be given here. The configuration of the coupled model with 60 km MetUM atmosphere,  $1/4^\circ$  NEMO ocean [Madec, 2014] resolution, and the CICE sea-ice model [Hunke *et al.*, 2015] is based on HadGEM3-GC2 [Williams *et al.*, 2015], with several alterations, and is hereby referred to as N216-O025. Given the interest in air-sea fluxes, the coupling period has been reduced to hourly (from 3 hourly) – note also that the ocean model has a 1 m thick top box. The primary comparison model is a 25 km atmosphere model coupled to the  $1/12^\circ$  NEMO ocean model (referred to as N512-O12), the configuration of the latter detailed in Hewitt *et al.* [2016], with all other settings as similar as possible to the lower resolution model. In particular, there was no tuning of the higher-resolution model – perhaps fortunately the top of atmosphere flux balance was little changed between the models [Hewitt *et al.*, 2016]. The initial ocean state for the models is from rest using the EN3 ocean analysis averaged over years 2004–2008 [Ingleby and Huddleston, 2007]. The atmosphere initial state is from a previous 25 km atmosphere-only simulation, regridded to the lower resolution.

The observational and reanalysis datasets used are as follows: wind speed from which wind stress is derived using the bulk formula for surface drag for neutral stability as developed by Large and Pond [1981] and modified by Trenberth *et al.* [1990] from both the Tropical Rainfall Measuring Mission satellite 2000–2008 (QuikSCATv4) [Ricciardulli *et al.*, 2011] and the cross-calibrated, multi-platform (CCMP), multi-instrument ocean surface wind velocity data set [Atlas *et al.*, 2011; NASA/GSFC/NOAA, 2009]; daily  $1/20^\circ$  SST (regridded as appropriate) from the ESA-CCI project [Merchant *et al.*, 2014] for 2000–2008; daily  $1/4^\circ$  NOAA-Optimum Interpolation Sea Surface Temperature (OISST) [Reynolds *et al.*, 2007]; daily  $1^\circ$  latent heat fluxes from the OAFlux dataset [Yu *et al.*, 2008] for 1985–2014; and monthly mean net surface heat flux product DEEP-C [Liu *et al.*, 2015] for 1985–2012 at  $0.7^\circ$  resolution, which employs a new methodology to estimate globally balanced net fluxes based on Top of Atmosphere observations and ERA-Interim energy divergence [after Trenberth *et al.*, 2001].

The spatial filtering of the daily fields has been performed using a box car filter with default scales of  $18^\circ$  longitude by  $6^\circ$  latitude. This is similar to the Loess filter used in the work of Maloney and Chelton [2006], Chelton and Xie [2010], and Bryan *et al.* [2010] but simpler to implement (Supporting information S1 provides algorithm and other details). To remove the spatially varying anomalies, each daily global field is high-pass spatially filtered and then monthly averaged. This allows only the stationary (mesoscale) anomalies to be retained. The monthly means are used both to derive some measure of linear regression fit (see later) and also for the temporal correlations. The individual months are averaged over multi-year seasons and extracted over the regions of interest. Text S1 documents more details and includes a comparison of output with previous studies.

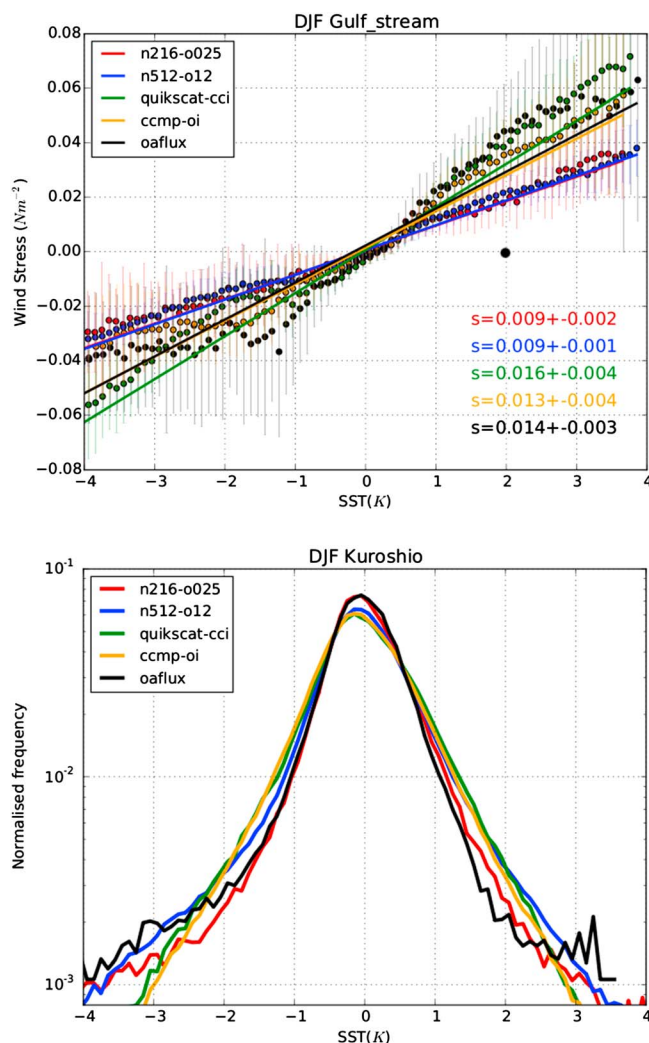


**Figure 1.** (top) Binned scatterplots of high-pass filtered SST and wind stress over the Gulf Stream region with the linear regression coefficient indicated (see Text S1). Red is the N216-O025 model, and blue is N512-O12. There are three pairs of observationally based data: ESA-CCI SST and QuikSCAT winds-stresses, OISST and CCMP wind stresses, and OAFlux surface temperature and wind stress. Error bars on the scatter plot are derived from the combined standard deviation of each monthly mean field, while for the regression the error is derived from the standard deviation of each monthly linear fit. (bottom) Normalized frequency of each SST bin for each dataset on a y-log scale.

stress (termed coupling coefficient) in December-January-February for the Gulf Stream from three different sources of observation/reanalysis data is 0.014–0.016 and agrees well with that from *Chelton and Xie* [2010] of 0.014 (the latter based on January-February data from QuikSCAT and Advanced Microwave Scanning Radiometer–EOS observations of SST). Notably, we include a wider SST range here but the results are comparable. Both N216-O025 and N512-O12 significantly underestimate the observed gradient by about 40%. This is due to underestimating the observed wind stress magnitudes, with little change between the two models. Most previous studies have shown differences when comparing  $\sim 1^\circ$  and  $\sim 1/10^\circ$  models in regions of strong mesoscale activity and favored the latter, while our results suggest that eddy-permitting resolution is sufficient to capture as much of the SST-wind stress relationship as seems to depend on model resolution.

Although the gradient is similar between models, Figure 1 (bottom) shows that the relative frequency of occurrence of each SST bin (normalized by the total number of points used in each dataset) does differ with resolution – the N512-O12 has two to three times more values at the positive extreme than N216-O025. Similarly, the OAFlux

### 3. Air-Sea Flux Relationships

Our initial analysis concentrates on the relationship of mesoscale perturbations in SST and wind stress. As discussed in *Chelton and Xie* [2010], at large scales there tends to be a negative correlation between SST and wind speed [Xie, 2004, and references therein], indicative of the ocean passively responding to wind-induced turbulent fluxes. At the mesoscale, however, the correlation becomes positive, implying that the associated ocean-atmosphere interactions are driven by spatial variations of SST.

The focus here is on the North Atlantic (other regions and methods are included in Text S1). Our analysis of air-sea interaction uses the high-pass spatially filtered fields of SST and wind stress in order to assess the relationship between mesoscale perturbations of these fields. As shown in previous studies [e.g., *Bryan et al.*, 2010; *Chelton and Xie*, 2010], it might be expected that the relationship will strengthen and better agree with observations as increased model resolution enables both sharper frontal structures and enhanced variability. Figure 1 (top) shows the SST-wind stress relationship over the Gulf Stream region ( $80^\circ\text{--}30^\circ\text{W}$ ,  $25^\circ\text{--}50^\circ\text{N}$ ). The values of the linear regression are included in Table S1.

The gradient in the linear regression between the binned SST and wind

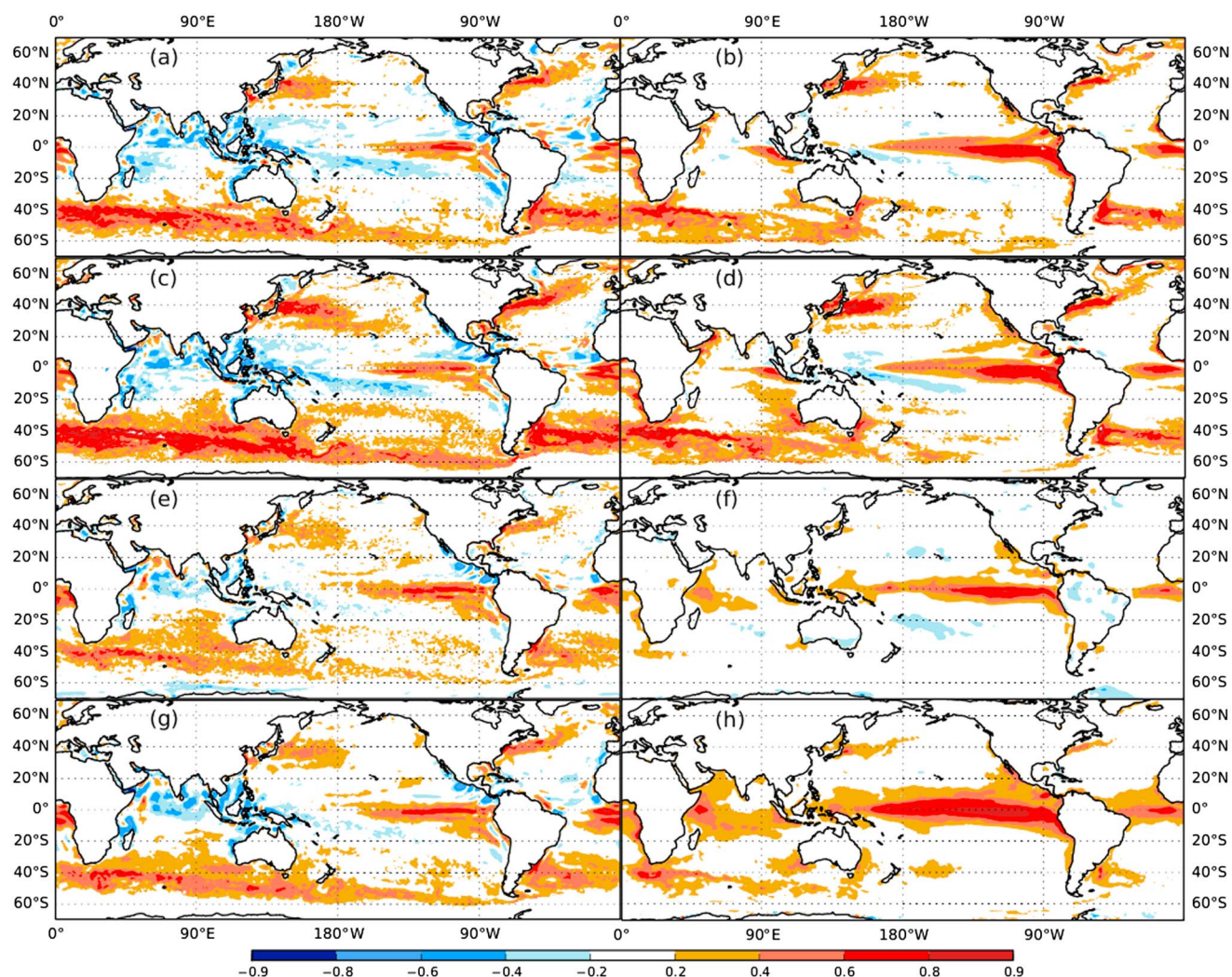


**Figure 2.** (left column) Correlation of the timeseries of monthly mean high-pass spatially filtered SST and wind stress derived from the daily data using all months. (right column) Correlation of temporal anomalies of monthly mean SST and total net surface heat flux (positive upwards). (a, b) N216-O025, (c, d) N512-O12, (e) OISST and CCMP wind stress, (f) OISST and DEEP-C net heat flux observations, (g) OAF flux surface temperature and wind stress and (h) OAF flux surface temperature and net heat flux observations. Hatching indicates significance at the 95% level.

dataset has fewer extreme values than the higher-resolution observational-based datasets. In regions where the SST and wind are correlated (see below), greater extremes could be expected to give rise to rectification of short-term mesoscale variability onto longer period variations of turbulent fluxes of heat, given that SST and wind product terms are involved in both the sensible and latent heat bulk formulations (see Text S3). The asymmetry in Figure 1 (bottom) between positive and negative SST seems to arise from the geography of the Gulf Stream and its coastline—other regions are more symmetric. To demonstrate that the relationships shown here are consistent with previous studies (given differences in both the data and filtering algorithms), in Text S1 the high pass spatial structure is shown over the Gulf Stream and Agulhas regions, comparable to Figure 1 of Chelton and Xie [2010] and Figure 2 of Bryan *et al.* [2010]. The SST-wind stress over the Kuroshio region has similar features as over the Gulf Stream, while in the Agulhas region the models agree better with observations with a small improvement at enhanced resolution—the latter may be due to the retroflexion in the Agulhas region and hence a different character compared to the lateral boundary in the Gulf Stream and Kuroshio.

The global-scale correlation between the monthly high-pass filtered SST and wind stress illustrates the temporal covariability between these fields. Bryan *et al.* [2010] showed that a  $1^\circ$  ocean model was not able to capture the observed relationship. Figures 2a, 2c, 2e, and 2g show that both N216-O025 and N512-O12 models capture all the regions of significant positive correlation seen in the observations. The only differences

between the models are enhanced correlation in the central northern Pacific, near boundary currents, and a larger region of high correlation in the Southern Ocean in N512-O12. In general, the model correlations are stronger than those seen in the observations, which implies that either the models are flawed or that observations are imperfectly sampling the climate. Corresponding correlations and regressions using only the winter hemisphere months are shown in Text S2, which suggests that much of the enhanced correlation in the eddy-resolving model originates in winter, perhaps related to the higher frequency of larger anomalies as seen in Figure 1 (bottom) and consequent stronger fluxes.

To complement understanding of the processes involved in covariability of SST and surface flux, we examine the correlation of temporal anomalies of monthly SST and turbulent flux. *Kirtman et al.* [2012] argue that regions of positive correlation are indicative of the ocean driving the atmosphere. The SST-heat flux correlations from models and observations are shown in Figures 2b, 2d, 2f, and 2h (the correlations are almost identical when using only latent heat flux). These agree well with those in *Kirtman et al.* [2012], with positive correlations strongly tied to boundary currents, the Antarctic Circumpolar Current and in the equatorial regions. For additional confirmation, the same correlation was calculated for the National Centers for Environmental Prediction–Climate Forecast System Reanalysis high-resolution reanalysis [*Saha et al.*, 2010] – this resembles the N216-O025 model in the tropics and Southern Hemisphere but in the Northern Hemisphere the correlations are only marginally higher than Figure 2h. Again, we find that the statistical relationships seen at eddy-resolving resolution (Figure 2 and *Kirtman*) are already achieved at eddy-permitting resolution.

Importantly, we also observe that the observationally-based datasets, particularly DEEP-C [*Liu et al.*, 2015], do not capture the mid-latitude correlations, suggesting either that the heat flux observations are insufficient to capture this variability (*Hyder et al.*, in preparation), or that the observed SST variability is under-represented. This has implications for how reliably observational datasets can be used to assess model processes. Further analysis of this temporal behaviour will be addressed in future work.

We note that the temporal correlations of SST-windstress and SST-heat flux are surprisingly similar given that they are derived from the two different methods and datasets. This suggests a dominant role for the turbulent heat flux anomalies which are directly or indirectly linked to SST and wind stress anomalies.

#### 4. Surface Fluxes and Heat Transports

The evidence presented above indicates that the 1/4° ocean is almost as good as the eddy-resolving model in representing air-sea fluxes, based on this limited set of common metrics. However, as shown in *Hewitt et al.* [2016], many aspects of the 1/12° coupled simulation mean state are significantly better, particularly in the North Atlantic and Southern Ocean. Here we attempt to explain these differences, and how the coupling strength assessed previously is implicated in them.

The annual mean surface heat flux from the DEEP-C dataset [*Liu et al.*, 2015] in the North Atlantic, together with the differences from OAFlex and models, is shown in Figure S4. The lack of heat loss to the south of the Gulf Stream in N216-O025 and related cold SST bias is a long-standing bias common to many models [*Wang et al.*, 2014]. The likely causes of the bias include the path of the North Atlantic Current (linked to separation of the Gulf Stream from the coast being typically too far north in lower resolution models) (*Chassignet and Marshall* [2008] and others), the magnitude of the ocean SST gradient [*Minobe et al.*, 2008], and having an adequate atmosphere resolution to properly respond to the SST gradients. In N512-O12 simulation the heat flux bias to DEEP-C is significantly reduced (though note the uncertainty in observationally based products in Figure S4b), equating to an average extra heat loss in this region of around  $1.5 \text{ W m}^{-2}$ . Examination of the model heat flux components reveals that the vast majority of this enhanced heat loss is in the latent heat. As shown in Text S3, using time-mean fields from the models, and a simple bulk formula [*Fairall et al.*, 2003] to calculate the turbulent heat fluxes, it can be shown that the increased latent heat loss, particularly south of the current path, is due to an increase in mean SST in the eddy-resolving model (of order  $1^\circ\text{C}$ ) – *Small et al.* [2014] also found the SST to dominate latent heat flux changes. The SST-latent heat flux relationship derived from spatial filtering (Text S3) agrees with this (i.e., a  $1^\circ\text{C}$  SST change equating to a heat flux of about  $20 \text{ W m}^{-2}$ ), and hence the reduction in heat flux bias is a combination of an improved SST mean state, together with a sufficiently strong atmosphere-ocean coupling strength to enable the enhanced heat

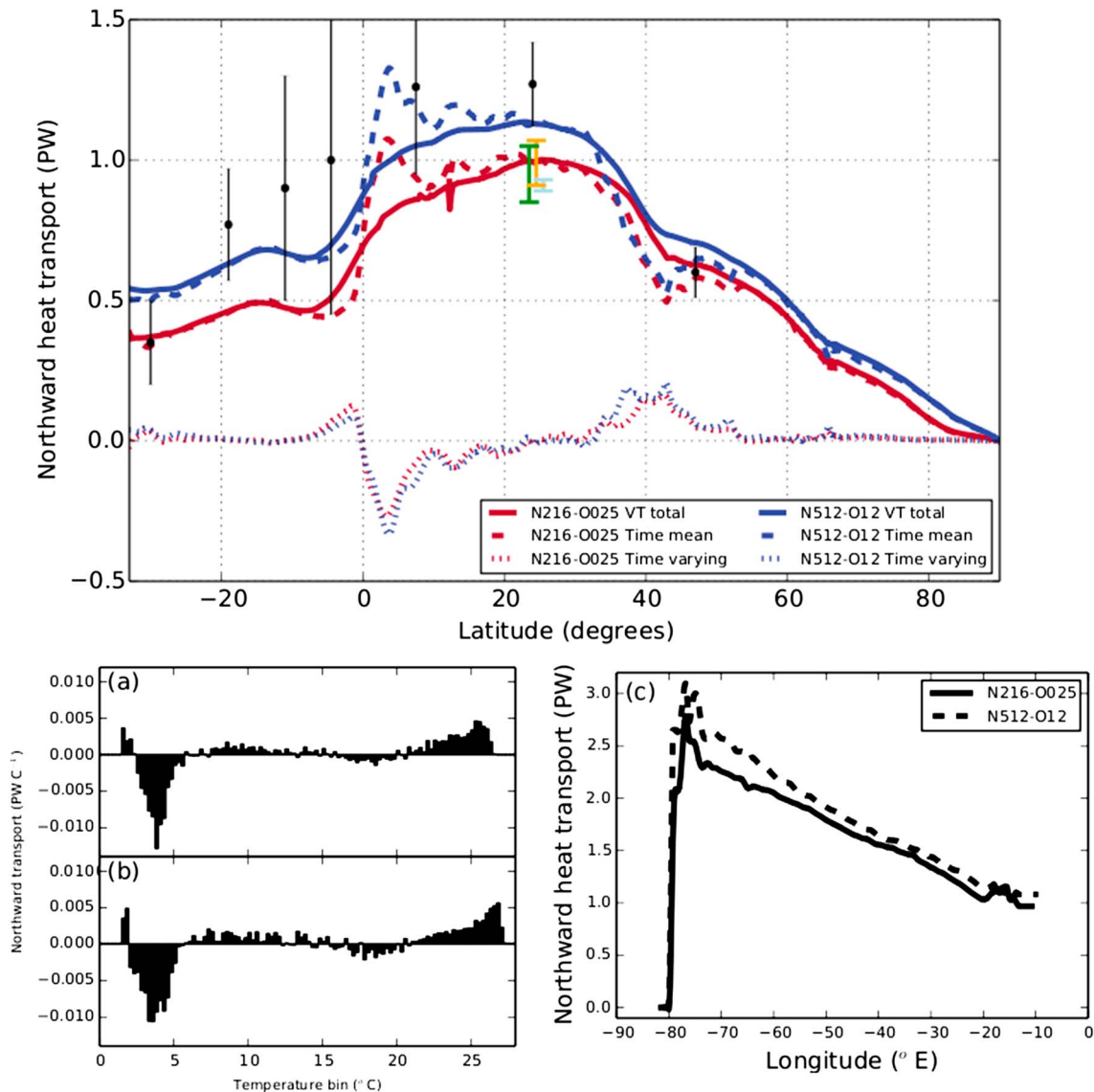


**Figure 3.** (top) Northward ocean heat transport in the North Atlantic from both models, together with observational estimates from *Ganachaud and Wunsch* [2003]. The colored bars indicate the range of heat transport from additional longer simulation (see text for details). Northward transport across 28°N split into temperature bins from (a) N216-O025 and (b) N512-O12. (c) Cumulative integral of northward heat transport across longitudes at 28°N for both models.

loss to the atmosphere. Better resolved interactions between ocean eddies and atmosphere, as shown by *Ma et al.* [2016], and enhanced synoptic forcing [*Wu et al.*, 2016] may also play an important role.

Accompanying the increased heat loss to the atmosphere in N512-O12 is an induced divergence in heat transport in the ocean, which drives an increase in ocean northward heat transport (Figure 3a). The N512-O12 simulation is in much better agreement with the observations [*Hewitt et al.*, 2016, Figure 4], and is associated with an increase in the meridional overturning circulation. Figures 3b and 3c show the transport in binned temperature classes across 28°N and the integral of the transport along 28°N, illustrating that the additional heat transport is accomplished at the highest temperatures within the boundary current. The N512-O12 simulation also has a slightly stronger southward heat transport at the colder (2–5 °C) temperatures. This demonstrates the key role of the boundary currents.

Conclusions drawn from only 20 years of simulation should be treated with caution, so for comparison we include in Figure 3 (top) the 5 year running mean maximum and minimum northward heat transport from 100 year simulations using the eddy-permitting ocean and 3-hourly coupling described in *Hewitt et al.* [2016] (GC2: green and GC2-N512: orange) and a 20 year N512-O025 simulation (light blue) parallel to those

described here. The N512-O12 mean remains outside the range from these longer simulations. The increased northward heat transport in N512-O12 is also associated with increased heat flux biases (Figure S4d) in the sub-polar gyre and Nordic/Arctic Seas due to warmer temperatures, possibly caused by addressing one part of a compensating error, while apparently lacking the required extra ocean heat loss farther north. Over longer timescales this would potentially impact the overturning circulation.

Hence, the combination of an adequate strength of the coupling between atmosphere and ocean (illustrated by the SST-wind stress relationship and already achieved in eddy-permitting model), together with an improved mean state in the eddy-resolving ocean (boundary current representation), combines together to generate improved surface fluxes.

## 5. Conclusions

This study has examined the air-sea flux relationships in eddy-resolving and eddy-permitting global coupled climate simulations, as well as changes to the mean state and the implications for the global large-scale circulation. We have shown that spatially high-pass filtered relationships between SST and wind stress are independent of ocean resolution in this study once that resolution is capable of representing the mesoscale adequately. To represent the mesoscale, it is necessary to permit eddies and/or adequate frontal structures and associated variability (the coupling period and ocean model vertical resolution may also be important). Both eddy-permitting and eddy-resolving models show a weaker relationship between SST and wind stress than observations. This is true across the three boundary current regions studied. The spatial pattern of correlation of the monthly mean high-pass spatial anomalies also agrees well, with boundary current and Southern Ocean regions having particularly high-temporal correlations. The strength of correlations is enhanced in the eddy-resolving model, showing the benefit of using multiple metrics to assess coupling strength. The same spatial correlation pattern is also shown to be much the same as that derived from correlations of monthly anomalies of SST and turbulent fluxes, as shown in *Kirtman et al.* [2012].

However, further analysis of the model mean state (following on from *Hewitt et al.* [2016]) reveals that the eddy-resolving ocean improves SST in the North Atlantic (partially due to the improved path of the North Atlantic Current), which produces a greatly enhanced latent heat loss to the atmosphere. The consequent increase in ocean heat transport divergence contributes to increased ocean northward heat transport and meridional overturning circulation, in much better agreement with observations.

Further understanding of the large-scale consequences of air-sea interactions, both in the mean and small-scale anomalies, will require more analysis. For example, isolating the mechanisms leading to increased SST in the eddy-resolving model to the south of the North Atlantic Current path and hence the reduced flux errors might suggest ways to improve eddy-permitting models or at least understand the consequences of their biases better. Studies such as *Ma et al.* [2015] suggest that representing small-scale SST variability can be important for the large-scale atmospheric circulation. To address this, coordinated experiments in which the SST is spatially filtered may help to isolate the robust aspects of such interactions [*Haarsma et al.*, 2016]. More reliable observations of turbulent fluxes on small space and timescales would enable a more robust assessment of model biases and help to disentangle model bias from observational uncertainty. A range of models may indicate whether the work by *Perlin et al.* [2014], which suggests that aspects of boundary layer parameterization may play a significant role in the strength of the coupling coefficient, is applicable.

Although this study does not include an ocean model of  $\sim 1^\circ$ , previous studies [e.g., *Bryan et al.*, 2010; *Kirtman et al.*, 2012] suggest that models of this resolution are fundamentally flawed in representing air-sea interactions. Unless methods are found to improve deficiencies in coupling, models with an eddy-permitting ocean, will be necessary to produce robust projections of climate variability and change.

The current practice for coupled climate change simulations, in which multicentennial simulations are required to reach a quasi-equilibrium state with small drift before anthropogenic forcing is applied, is indicative of missing processes (biogeochemical processes excepted). These results suggest that improved process representation may be able to dramatically reduce climate drift and enable models to maintain states more similar to that observed.

There are some key weaknesses of this study that can be addressed in future work: 20 years of parallel simulation is clearly shorter than ideal (given initial model drifts) to study the long term climate circulation,

though it is more than sufficient for the daily air-sea interactions, and only one configuration of one model is used. Both of these will be addressed by the European Union Horizon 2020 project PRIMAVERA, involving 19 European groups – this will assess the robustness of results shown here by producing a multi-model ensemble of eddy-resolving coupled simulations, each of hundred years in length, using the same integration protocol. Such simulations will be compared to lower resolution counterparts (as part of the Coupled Model Intercomparison Project Phase 6 (CMIP6) HighResMIP protocol) [Haarsma *et al.*, 2016] to better understand climate processes that are either missing or poorly represented in typical climate model configurations.

## Acknowledgments

This work was supported by the Joint UK DECC/Defra Met Office Hadley Centre Climate Programme (GA01101) and part funded through the PRIMAVERA project under Grant Agreement 641727 in the European Commission's Horizon 2020 research programme. We acknowledge use of the MONSooN system, a collaborative facility supplied under the Joint Weather and Climate Research Programme, which is a strategic partnership between the Met Office and the Natural Environment Research Council. The author also acknowledges support from the EU FP7 project IS-ENES2 for work on ESMF and regridding tools. We wish to thank STFC CEDA for use of the JASMIN storage and analysis platform along with the corresponding support teams. We also thank the many people involved in model development, simulation, and analysis of these large datasets. We would like to thank R. Justin Small and an anonymous reviewer for their insightful comments which helped to strengthen the manuscript, and useful discussions with Jeremy Grist. QuikScat data are produced by Remote Sensing Systems and sponsored by the NASA Ocean Vector Winds Science Team. Data are available at [www.remss.com](http://www.remss.com). CCMP data product Atlas FLK v1.1 derived surface winds (level 3.0) available from [https://podaac.jpl.nasa.gov/Cross-Calibrated\\_Multi-Platform\\_OceanSurfaceWindVectorAnalyses](https://podaac.jpl.nasa.gov/Cross-Calibrated_Multi-Platform_OceanSurfaceWindVectorAnalyses). The global ocean heat flux and evaporation products were provided by the WHOI OaFlux project (<http://oafux.whoi.edu>) funded by the NOAA Climate Observations and Monitoring (COM) program. Further details of the DEEP-C heat flux product [Liu *et al.*, 2015] are available from <http://www.met.rdg.ac.uk/~sgs02rpa/research/DEEP-C/GRL/>, funded by the Natural Environment Research Council DEEP-C grant NE/K005480/1. Due to the size of the model datasets needed for the analysis (global, daily SST, wind stress and heat fluxes on 60 km and 25 km grids over 20 years) they require large storage space of order 1 TB. They can be shared via the STFC-CEDA platform JASMIN by contacting the author.

## References

- Atlas, R., R. N. Hoffman, J. Ardizzone, S. M. Leidner, J. C. Jusem, D. K. Smith, and D. Gombos (2011), A cross-calibrated, multiplatform ocean surface wind velocity product for meteorological and oceanographic applications, *Bull. Am. Meteorol. Soc.*, **92**, 157–174, doi:10.1175/2010BAMS2946.1.
- Bryan, F. O., R. Tomas, J. M. Dennis, D. B. Chelton, N. G. Loeb, and J. L. McClean (2010), Frontal scale air-sea interaction in high-resolution coupled climate models, *J. Clim.*, doi:10.1175/2010JCLI3665.1.
- Chassignet, E. P., and D. P. Marshall (2008), Gulf Stream Separation in Numerical Ocean Models, in *Ocean Modeling in an Eddy Regime*, edited by M. W. Hecht and H. Hasumi, AGU, Washington, D. C., doi:10.1029/177GM05.
- Chelton, D. B., and S.-P. Xie (2010), Coupled ocean-atmosphere interaction at oceanic mesoscales, *Oceanography*, **23**(4), 52–69.
- Chelton, D. B., M. G. Schlax, M. H. Freilich, and R. F. Milliff (2004), Satellite measurements reveal persistent small-scale features in ocean winds, *Science*, **303**, 978–983.
- Chelton, D. B., M. G. Schlax, and R. M. Samelson (2007), Summertime coupling between sea surface temperature and wind stress in the California current system, *J. Phys. Oceanogr.*, **37**, 495–517.
- Fairall, C. W., E. F. Bradley, J. E. Hare, A. A. Grachev, and J. B. Edson (2003), Bulk parameterization on air-sea fluxes: Updates and verification for the COARE algorithm, *J. Clim.*, **16**, 571–591.
- Ganachaud, A., and C. Wunsch (2003), Large-scale ocean heat and freshwater transports during World Ocean Circulation Experiment, *J. Clim.*, **16**, 696–705.
- Haarsma, R. J., et al. (2016), High Resolution Model Intercomparison Project (HighResMIP), *Geosci. Model Dev. Discuss.*, doi:10.5194/gmd-2016-66.
- Hallberg, R. (2013), Using a resolution function to regulate parameterizations of oceanic mesoscale eddy effects, *Ocean Modell.*, **72**, 92–103, doi:10.1016/j.ocemod.2013.08.007.
- Hewitt, H. T., et al. (2016), The impact of resolving the Rossby radius at mid-latitudes in the ocean: Results from a high-resolution version of the Met Office GC2 coupled model, *Geosci. Model Dev. Discuss.*, doi:10.5194/gmd-2016-87.
- Hunke, E. C., W. H. Lipscomb, A. K. Turner, N. Jeffery, and S. Elliott (2015), CICE: The Los Alamos Sea Ice Model, Documentation and Software User's Manual, Version 5.1. Tech. Rep. LA-CC-06-012, Los Alamos National Laboratory, Los Alamos, New Mexico. [Available at <http://oceans11.lanl.gov/trac/CICE>.]
- Ingleby, B., and M. Huddleston (2007), Quality control of ocean temperature and salinity profiles - Historical and real-time data, *J. Mar. Syst.*, **65**, 158–175.
- Kirtman, B. P., et al. (2012), Impact of ocean model resolution on CCSM climate simulations, *Clim. Dyn.*, **39**, 1303–1328, doi:10.1007/s00382-012-1500-3.
- Large, W. G., and S. Pond (1981), Open ocean momentum flux measurements in moderate to strong winds, *J. Phys. Oceanogr.*, **11**, 324–336.
- Liu, C., R. P. Allan, P. Berrisford, M. Mayer, P. Hyder, N. Loeb, D. Smith, P.-L. Vidale, and J. M. Edwards (2015), Combining satellite observations and reanalysis energy transports to estimate global net surface energy fluxes 1985–2012, *J. Geophys. Res. Atmos.*, **120**, 9374–9389, doi:10.1002/2015JD023264.
- Ma, X., P. Chang, R. Saravanan, R. Montuoro, J.-S. Hsieh, D. Wu, X. Lin, L. Wu, and Z. Jing (2015), Distant Influence of Kuroshio Eddies on North Pacific Weather Patterns?, *Sci. Rep.*, **5**, 17785, doi:10.1038/srep17785.
- Ma, X., et al. (2016), Western boundary currents regulated by interaction between ocean eddies and the atmosphere, *Nature*, **535**, 533–537, doi:10.1038/nature1864.
- Madec, G. (2014), "NEMO ocean engine". Note du Pôle de modélisation, Institut Pierre-Simon Laplace (IPSL), France.
- Maloney, E. D., and D. B. Chelton (2006), An assessment of the sea surface temperature influence on surface wind stress in numerical weather prediction and climate models, *J. Clim.*, **19**, 2743–2762.
- Merchant, C. J., et al. (2014), Sea surface temperature datasets for climate applications from Phase 1 of the European Space Agency Climate Change Initiative (SST CCI), *Geosci. Data J.*, **1**, 179–191, doi:10.1002/gdj3.20.
- Minobe, S., A. Kuwano-Yoshida, N. Komori, S.-P. Xie, and R. J. Small (2008), Influence of the Gulf Stream on the troposphere, *Nature*, **452**, doi:10.1038/nature06690.
- NASA/GSFC/NOAA (2009), Cross-Calibrated Multi-Platform Ocean Surface Wind Vector L3.0 First-Look Analyses Ver. 1. PO.DAAC, Calif. Dataset accessed [2016-02-01] at. [Available at 10.5067/CCF30-01XXX.]
- Perlin, N., S. P. de Zoete, D. B. Chelton, R. M. Samelson, E. D. Skillingstad, and L. W. O'Neill (2014), Modeling the atmospheric boundary layer wind response to mesoscale sea surface temperature perturbations, *Mon. Weather Rev.*, **142**, 4284–4307.
- Reynolds, R. W., T. M. Smith, C. Liu, D. B. Chelton, K. S. Casey, and M. G. Schlax (2007), Daily high-resolution-blended analyses for sea surface temperature, *J. Clim.*, **20**, 5473–5496.
- Ricciardulli, L., F. J. Wentz, and D. K. Smith (2011), Remote Sensing Systems QuikSCAT Ku-2011 Daily, Ocean Vector Winds on 0.25 deg grid, Version 4. Remote Sensing Systems, Santa Rosa, Calif. [Available at [www.remss.com/missions/quikscat](http://www.remss.com/missions/quikscat).]
- Saha, S., et al. (2010), The NCEP climate forecast system reanalysis, *Bull. Am. Meteorol. Soc.*, **91**, 1015–1057, doi:10.1175/2010BAMS3001.1.
- Scaife, A. A., D. Copsey, C. Gordon, C. Harris, T. Hinton, S. J. Keeley, A. O'Neill, M. Roberts, and K. Williams (2011), Improved Atlantic Blocking in a Climate Model, *Geophys. Res. Lett.*, **38**, L23703, doi:10.1029/2011GL049573.
- Small, R. J., et al. (2014), A new synoptic-scale resolving global climate simulation using the Community Earth System Model, *J. Adv. Model. Earth Syst.*, **6**, 1065–1094, doi:10.1002/2014MS000363.
- Trenberth, K. E., W. G. Large, and J. G. Olson (1990), The mean annual cycle in global ocean wind stress, *J. Phys. Oceanogr.*, **20**, 1742–1760.

- Trenberth, K. E., J. M. Caron, and D. P. Stepaniak (2001), The atmospheric energy budget and implications for surface fluxes and ocean heat transports, *Clim. Dyn.*, *17*, 259–276.
- Wang, C., L. Zhang, S.-K. Lee, L. Wu, and C. R. Mechoso (2014), A global perspective on CMIP5 climate model biases, *Nat. Clim. Change*, *4*, 201–205, doi:10.1038/nclimate2118.
- Williams, K. D., et al. (2015), The Met Office Global Coupled model 2.0 (GC2) configuration, *Geosci. Model Dev.*, *8*, 1509–1524, doi:10.5194/gmd-8-1509-2015.
- Wu, Y., X. Zhai, and Z. Wang (2016), Impact of Synoptic Atmospheric Forcing on the Mean Ocean Circulation, *J. Clim.*, *29*, 5709–5724, doi:10.1175/JCLI-D-15-0819.1.
- Xie, S.-P. (2004), Satellite observations of cool ocean–atmosphere interaction, *Bull. Am. Meteorol. Soc.*, *85*, 195–208.
- Yu, L., X. Jin, and R. A. Weller (2008), Multidecade Global Flux Datasets from the Objectively Analyzed Air-sea Fluxes (OAFlux) Project: Latent and sensible heat fluxes, ocean evaporation, and related surface meteorological variables, *OAFlux Project Tech. Rep.*, OA-2008-01, 64 pp., Woods Hole Oceanogr. Inst., Woods Hole, Mass.
- Zhang, Y., and G. K. Vallis (2013), Ocean Heat Uptake in Eddying and Non-Eddying Ocean Circulation Models in a Warming Climate, *J. Phys. Oceanogr.*, *43*(10), 2211–2229, doi:10.1175/JPO-D-12-078.1.